Pharm Res (2012) 29:2722–2737
DOI 10.1007/s11095-011-0591-6

RESEARCH PAPER

Kinetics and Mechanisms of Deamidation and Covalent Amide-Linked Adduct Formation in Amorphous Lyophiles of a Model Asparagine-Containing Peptide

Michael P. DeHart • Bradley D. Anderson

Received: 5 April 2011 / Accepted: 13 September 2011 / Published online: 18 October 2011

ABSTRACT

Purpose Asparagine containing peptides and proteins undergo deamidation via a succinimide intermediate. This study examines the role of the succinimide in the formation of covalent, amide-linked adducts in amorphous peptide formulations.

Methods Stability studies of a model peptide, Gly-Phe-L-Asn-Gly, were performed in lyophiles containing an excess of Gly-Val at 'pH' 9.5 and 40°C/40% RH. Reactant disappearance and the formation of ten different degradants were monitored by HPLC. Mechanism-based kinetic models were used to generate rate constants from the concentration *vs*. time profiles.

Results Deamidation of Gly-Phe-L-Asn-Gly in lyophiles resulted in L- and D-aspartyl and isoaspartyl-containing peptides and four amide-linked adducts between the succinimide and Gly-Val. The kinetic analysis demonstrated competition between water and terminal amino groups in Gly-Val for the succinimide. The extent of covalent adduct formation was dependent on dilution effects due to its second order rate law.

Conclusion The cyclic imide formed during deamidation of asparagine containing peptides in lyophiles can also lead to covalent adducts due to reaction with other neighboring peptides. A reaction model assuming a central role for the succinimide in the formation both hydrolysis products and covalent adducts was quantitatively consistent with the kinetic data. This mechanism may contribute to the presence of covalent, non-reducible aggregates in lyophilized peptide formulations.

M. P. DeHart • B. D. Anderson (✉)
Department of Pharmaceutical Sciences, College of Pharmacy
University of Kentucky
A323A ASTeCC Bldg.
Lexington, Kentucky 40536-0082, USA
e-mail: bande2@email.uky.edu

KEY WORDS aggregation · amorphous reaction kinetics · covalent adducts · deamidation · lyophilization

INTRODUCTION

The chemical and physical instability of proteins and peptides in aqueous formulations has been a topic of considerable interest in the pharmaceutical literature and the subject of several excellent reviews (1–4). Generally, the chemical instability of proteins and peptides can be attributed to specific amino acid side chains and sequences that are particularly likely to participate in chemical reactions, such as residues that contain reactive amine or thiolate nucleophiles (e.g., lysine or cysteine) (5,6), residues prone to oxidation (e.g., methionine, cysteine, histidine, tryptophan, and tyrosine) (7–9), or cystine residues that are susceptible to thiol-disulfide exchange or β-elimination reactions that can lead to reducible or non-reducible aggregate formation (5,6,10,11). Of the numerous so-called "hot spots" demarcating locations particularly prone to chemical degradation, asparagine and to a lesser extent glutamine residues are among the most frequently involved (12–14). Side-chain deamidation, peptide backbone isomerization, and racemization reactions occurring at asparagine and glutamine residues in proteins and peptides all appear to be linked to the formation of a reactive cyclic imide intermediate (15,16). At asparagines, formation of a reactive five-membered succinimide ring is the result of a nucleophilic attack by the adjacent backbone amide nitrogen on the C-terminus side at the amide side-chain, accompanied by the liberation of ammonia (hence, deamidation). The reactive cyclic imide intermediate can be attacked by a molecule of water at either carbonyl, leading to aspartate or isoaspartate-containing degradation products. In aqueous solution,

isoaspartate formation in peptides is usually preferred by approximately 3:1 (15,17) but this ratio depends on the solvent (18,19) and local microenvironment (20–22). Racemization at the α-carbon of asparagine also occurs, and has been linked to the enhanced acidity of the hydrogen on the α-carbon in the succinimide intermediate (15), though tetrahedral intermediates along the reaction coordinate may also undergo racemization (23).

While the central role of cyclic imide intermediates in the reactions summarized above is widely recognized, the enhanced susceptibility of this intermediate to nucleophilic attack raises the possibility that other degradants may arise from reactions with nucleophiles other than water (24). In the case of insulin, deamidation of the asparagine residue at the A-21 terminus in aqueous solutions leads to parallel formation of covalent amide-linked dimers (25–27). However, both deamidation and covalent dimer formation at the A-21 position of insulin were shown to proceed through a highly reactive cyclic anhydride rather than a cyclic imide intermediate, with covalent dimers stemming from the intermolecular attack of primary amino groups in neighboring insulin molecules on the anhydride. Competition between water and protein amino groups for reaction with the cyclic anhydride was also observed in amorphous lyophile formulations, where the relative amounts of degradants produced depended on various formulation factors including protein concentration, water content, and apparent pH (28–30).

In a recent publication from these laboratories, we demonstrated the potential for Asn-containing proteins and peptides to generate a more diverse set of degradants due to the reaction of nucleophilic amines with a succinimide intermediate (24). The decomposition kinetics of the tripeptides Phe-Asn-Gly and Phe-isoAsn-Gly in aqueous solutions ranging from pH 8.5–10.5 indicated that, in addition to deamidation to form isoAsp and Asp peptides in a ratio of approximately 3:1, cis-and trans-diketopiperazines were produced via intramolecular attack of the peptide amino terminus on the succinimide. The formation of both cis- and trans-isomers was attributed to partial racemization of the cyclic imide or a precursor prior to formation of the diketopiperazine. In ammonia containing buffers, Phe-Asn-Gly and Phe-isoAsn-Gly isomerization was demonstrated as the result of the back reaction of ammonia with the succinimide intermediate. These observations established the plausibility that a wide range of heretofore unidentified degradants may form via intra- or intermolecular attack by nucleophilic amines at cyclic imide intermediates generated during Asn or Gln deamidation or Asp isomerization reactions, even in aqueous solutions.

In amorphous lyophiles of Asn-containing peptides or their mixtures with polymeric excipients, deamidation proceeds through cyclic imide formation as in aqueous solution but the product distribution (isoAsp/Asp ratio) and kinetics are altered depending on water content (3,31–33). Recently, Desfougères *et al.* (34) prepared hen egg-white lysozyme with variable numbers of succinimide residues by heating lysozyme powder freeze-dried from pH 3.5 solutions (pH conditions that favor succinimide formation from Asp residues) for up to 7 days at 80°C. Under these conditions, the sites that were converted to succinimides were identified as Asp18, Asp48, Asp66, Asp101, and Asn103. Using SDS-PAGE to detect covalent dimer formation, they demonstrated a linear relationship between the quantity of dimeric species and the % of succinimide in the derivatives. The mechanism proposed to account for these results was one in which nucleophilic attack of an amine containing side-chain (i.e., lysine) in one molecule occurred on either of the two carbonyl carbons in a succinimide intermediate present on an adjacent molecule. Thus, there is growing evidence that lyophilized formulations of proteins and peptides that contain Asn, Gln, or Asp residues may degrade to form covalent dimers, trimers, and other aggregates via reactive cyclic imide intermediates.

The aim of the present study is to test the following hypotheses: a) covalent, amide-linked adducts can form in amorphous lyophiles from the intermolecular reaction of primary amine nucleophiles in neighboring peptide molecules with Asn-containing peptides; and b) adduct formation occurs through a reactive cyclic imide intermediate. The model peptides chosen for this study were Gly-Phe-L-Asn-Gly along with the D- and L-cyclic imides, Gly-Phe-L-Asu-Gly and Gly-Phe-D-Asu-Gly. If the above hypotheses are correct, lyophiles containing only the tetrapeptide Gly-Phe-L-Asn-Gly should have a tendency to form amide-linked dimers, trimers, tetramers, and higher order aggregates as well as their isomers and racemates. Therefore, to reduce the number of possible degradants likely to form, kinetic studies of Gly-Phe-L-Asn-Gly degradation were conducted in the presence of an excess of Gly-Val. Because both Gly-Val and any amide-linked covalent adducts produced between these two peptides would no longer contain an Asn residue, they were expected to have a reduced tendency to form higher order aggregates.

MATERIALS AND METHODS

Chemicals and Reagents

The peptides Gly-Phe-L-Asn-Gly (95.4%), Gly-Phe-D-Asp-Gly (99.5%), Gly-Phe-L-Asp-Gly (99.5%), Gly-Phe-D-isoAsp-Gly (97.2%), and Gly-Phe-L-isoAsp-Gly (99.5%) were synthesized by GenScript (Piscataway, NJ) and provided as their trifluoroacetate (TFA) salts. The percentages listed in parentheses are HPLC purities determined at 220 nm as reported in certificates of analysis from GenScript. Purities were also assessed by comparing peak areas of each peptide to

phenylalanine (Sigma, purity >99% by TLC) standards at 257 nm since phenylalanine is the only amino acid contributing to the UV absorbance at this wavelength. The polymer, hypromellose, (HPMC, Methocel E5) was a donated by Dow Chemical (Midland, MI) and used as received. The dipeptide Gly-Val was purchased from Bachem (Torrance, CA) as the zwitterion (purity 99.0% by TLC). Acetonitrile was HPLC grade and purchased from Fisher Scientific (Springfield, NJ). Sodium bicarbonate (ACS grade) was purchased from EM Science (Gibbstown, NJ) and succinic acid was purchased from Aldrich (St. Louis, MO). Deionized water was used for all experiments.

Cyclic Imide Synthesis

The D- and L- forms of the cyclic imide intermediates, Gly-Phe-L-Asu-Gly and Gly-Phe-D-Asu-Gly, were synthesized by incubating the corresponding aspartate (~3–4 mg) in a 9:1 mixture of acetic acid and hydrochloric acid (2 mL) for 2 days (35,36). The desired product was purified by HPLC using a Waters Alliance LC system with the autosampler at 4°C, a Supelcosil ABZ+ column (15 cm×3.5 mm, 5-μm pore size), and a mobile phase consisting of 5% acetonitrile and 95% water adjusted to pH 4.1 with acetic acid. Peaks containing the succinimide were collected in a 20-mL scintillation vial, frozen overnight at −20°C, and freeze-dried at 0°C under a vacuum (100 mtorr) for 2 days. Approximately 1.5 mg of a fluffy, white powder was obtained and stored in a dessicator at −20°C.

Purity of the L-succinimide was determined by overnight hydrolysis of an accurately weighed sample in an aqueous solution at pH 10.5 and ambient temperature. The pH of the hydrolyzed sample was lowered to 4.0–4.2 with hydrochloric acid (1 N) and analyzed by HPLC (see HPLC Analyses). Complete hydrolysis of the L-succinimide resulted in the formation of D- and L-isoaspartates and aspartates, the amounts of which were determined from peak areas using synthetic standards. By comparing the total quantity of hydrolysis products generated to the initial quantity of succinimide, the imide purity was determined to be 97.2%± 1.1% (n=2). HPLC response factors of the D- and L-succinimides were assumed to be the same. Therefore, the L-succinimide was used as a standard to represent both.

Covalent Adduct Syntheses

Covalent adducts between Gly-Phe-L-Asn-Gly or Gly-Phe-D-Asn-Gly and Gly-Val were formed in lyophiles prepared from 0.2 mM Gly-Phe-L-Asu-Gly or Gly-Phe-D-Asu-Gly solutions containing a 30-fold molar excess of Gly-Val and adjusted to pH 9.5 with NaOH. Aliquots were transferred into sample vials, immediately frozen, and lyophilized. The lyophiles were then incubated at 40°C and 40% relative humidity (RH) for 6 h and stored in a freezer (−20°C) under dessicant for later analysis by HPLC or mass spectrometry.

Preparation of Gly-Phe-L-Asn-Gly and Gly-Phe-Asu-Gly Lyophiles for Kinetic Analyses

Gly-Phe-L-Asn-Gly solutions (1 mM) were prepared by adding approximately 1 mg of the TFA salt of Gly-Phe-L-Asn-Gly to 2 mL of a solution containing HPMC (10 mg), and either a combination of 2.6 mg Gly-Val and 7.8 mg sodium bicarbonate (formulation A) or 10.5 mg Gly-Val (formulation B) adjusted to pH 9.5 with dilute sodium hydroxide. The compositions of formulations A and B are listed in Table I. To examine variability between formulation preparations, formulation A was prepared in duplicate and exposed to the same storage conditions. When the starting reactant was either the D- or L-cyclic imide, 150 μg of the respective peptide was added to 2 mL of the same buffer/polymer solution described above (final concentration of cyclic imide was ~0.2 mM). The solutions were mixed and 100 μL aliquots were transferred into glass autosampler vials. Vials were immediately placed on a pre-chilled lyophilization shelf (−45°C) for approximately 5–8 min to freeze the samples after which the lyophilization cycle was initiated. Lyophilization was performed on a Virtis Advantage (Stoneridge, NY) tray dryer and the cycle consisted of primary drying at −40°C for 1420 min followed by a ramp to 40°C in 180 min and secondary drying at 40°C for 120 min. The pressure was held constant at 100 mtorr throughout the cycle.

Kinetic Studies

Lyophiles containing Gly-Phe-L-Asn-Gly were pre-equilibrated at 40% RH (over saturated potassium carbonate solution) and ambient temperature for 12 h then placed in a dessicator at the same relative humidity and 40°C. Lyophiles containing either Gly-Phe-L-Asu-Gly or Gly-Phe-D-Asu-Gly formulations were placed directly in a desiccator at 27°C and 75% RH. These storage conditions were chosen due to a reduced rate of degradation for the succinimide and to ensure that all eight degradants are observed with the succinimide. At predetermined time intervals, individual sample vials were removed from the incubation chamber, reconstituted with deionized water, and the pH was adjusted with 1 N hydrochloric acid (~4–6 μL) to pH 4.1 to match the mobile phase and to limit further degradation. Samples were either analyzed immediately by HPLC or stored in a −20°C freezer until analysis. Both the disappearance of starting peptide and initial rates of formation of degradants were monitored.

For kinetic analyses, only data up to 25% disappearance of the starting peptide were utilized, as in this region

Table I Composition of Gly-Phe-L-Asn-Gly Lyophile Formulations Prepared for Kinetic Studies. Water Contents Measured are Post-Lyophilization and at the End of the Kinetic Study After Correction for the Carbonate Contribution to Apparent Water Content

Ingredient	Formulation A (~8× Gly-Val molar excess)		Formulation B (~30× Gly-Val molar excess)	
	w/w	moles/L[a]	w/w	moles/L[a]
Gly-Phe-L-Asn-Gly	2.92%	0.096	2.94%	0.098
Gly-Val	9.88%	0.738	39.2%	2.93
Carbonate	21.5%	–	–	–
Sodium	9.27%	–	4.46%	–
HPMC	39.5%	–	38.5%	–
TFA	0.895%	–	0.902%	–
Water content:				
Initial	2.4 ± 0.6%	–	3.5 ± 0.7%	–
@ 40% RH	16.9 ± 1.6%	–	14.0 ± 1.7%	–
pH[b]	9.56		9.60	

[a] molar concentrations were estimated by assuming a solid density of 1.3 g/mL

[b] pH after reconstitution in deionized water

degradant concentrations increased linearly with time and mass balances >95% were maintained. Individual peak areas for all hydrolysis products, L- or D-succinimides and covalent adducts were pooled and labeled as either "Aspartates," "Imides," or "Adducts," respectively. Differential equations based on the pathways depicted in Fig. 1 were derived to fit the concentration *versus* time profiles (Eqs. 1–4). Figure 1 illustrates the formation of the succinimide intermediate from Gly-Phe-L-Asn-Gly followed by its subsequent breakdown to either aspartates or covalent Gly-Val adducts. Fits were performed by non-linear least squares regression analysis using commercially available computer software (Scientist, Micromath Scientific Software, St. Louis, MO). Data from the duplicate preparations of formulation A were fit simultaneously using the same rate constants for parallel reaction pathways in the two formulations.

$$\frac{d[GFNG]}{dt} = -k_{imide}[GFNG] \quad (1)$$

$$\frac{d[imide]}{dt} = k_{imide}[GFNG] - k_{aspartates}[imide] - k_{adduct}[imide] \quad (2)$$

$$\frac{d[Aspartates]}{dt} = k_{aspartates}[imide] \quad (3)$$

$$\frac{d[Adducts]}{dt} = k_{adduct}[imide] \quad (4)$$

HPLC Analyses

Separation of Gly-Phe-L-Asn-Gly and its degradants was performed on a Waters Alliance LC system with the autosampler set at 4°C using a Supelcosil ABZ+ column (15 cm×3.5 mm, 5-µm pore size) and a mobile phase consisting of 100% aqueous buffer (20 mM succinic acid,

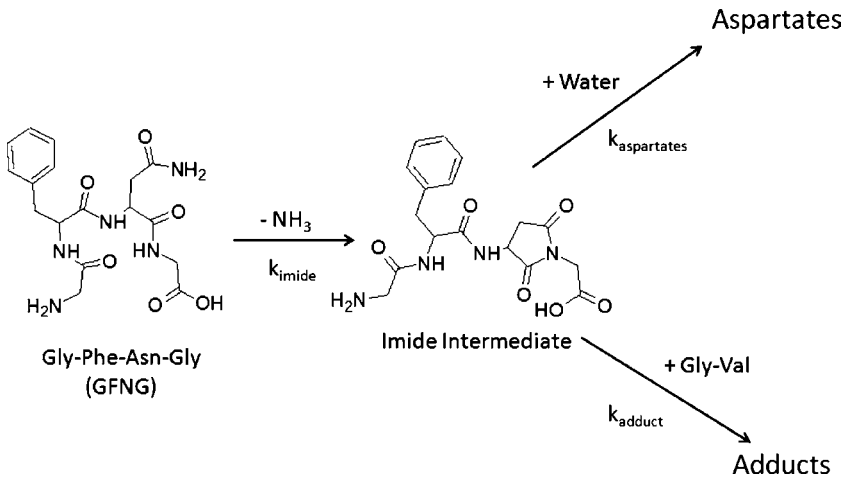

Fig. 1 Simplified model used to generate rate constants for the formation of the succinimide intermediate from Gly-Phe-L-Asn-Gly, imide hydrolysis to form aspartates, and covalent adduct formation from the reaction the succinimide with Gly-Val.

pH 4.1) for 16 min followed by a step gradient to 5:95 acetonitrile:buffer for 19 min at 1.6 mL/min with UV detection at 220 and 257 nm. Each injection was followed by a wash (75:25 acetonitrile:buffer for 5 min) and a 15 min re-equilibration to 100% aqueous buffer.

Concentrations of Gly-Phe-L-Asn-Gly, succinimides and hydrolysis products were determined by comparison of peak areas at 220 nm to those of reference standards at the same wavelength after adjusting standard concentrations for their purity. Purities of the L- and D-succinimide reference standards were determined from the amounts of aspartate products produced on hydrolysis in aqueous solution as described above while the purities of Gly-Phe-L-Asn-Gly and all hydrolysis product reference standards were determined from response factors at 257 nm relative to phenylalanine. Covalent adduct response factors at 220 nm relative to Gly-Phe-L-Asn-Gly were determined by reconstituting lyophilized covalent adduct mixtures (see Covalent Adduct Syntheses) with a stock solution containing a known concentration of Gly-Phe-L-Asn-Gly and analyzing by HPLC at both 220 and 257 nm. Peak areas of adducts were converted to concentrations by assuming that adducts have the same molar absorbance at 257 nm as Gly-Phe-L-Asn-Gly due to the presence of one phenylalanine in each. The calculated adduct concentration was then used to convert peak areas at 220 nm to adduct response factors relative to Gly-Phe-L-Asn-Gly. These relative response factors were then used to determine the amounts of adducts present in samples being monitored during stability studies.

Mass Spectrometry

Four adduct peaks were detected by HPLC and collected for tandem mass spectrometry to determine their molecular weights and primary sequence information. The peaks were isolated using a mobile phase consisting of 80 mM formic acid adjusted to pH 4.1 with ammonium hydroxide and the same HPLC system described above, concentrated under a nitrogen flow, re-diluted 10× in acetonitrile/water (1:1), and introduced by a syringe pump at 3 μL/min into a Finnigan LCQ ion trap mass spectrometer using electrospray ionization (ESI) in the positive ion mode as the method of detection.

Lyophile Characterization

Water Content

Lyophiles were analyzed for water content post-lyophilization and at the end of the kinetic experiments by a Karl-Fischer titration (Metrohm, Riverview, FL). Samples (15 mg) were dissolved in approximately 400–600 μL of anhydrous dimethylsulfoxide (DMSO, Acros Organics, Morris Plains, NJ) for analysis and the water determined from the same volume of a DMSO blank was subtracted. Samples were analyzed in triplicate and the average value is reported.

Reconstituted Solution pH

Lyophiles were reconstituted with the original fill volume (100 μL) of deionized water both at the beginning and end of kinetic experiments. pH measurements were taken using a MI-40 combination micro-pH probe (Microelectrodes, Inc., Bedford, NH) attached to a Beckman pHI 40 pH Meter (Brea, CA).

Polarized Light Microscopy

Lyophile formulations A and B were analyzed by polarized light microscopy post-lyophilization and after incubation at 40°C and 40% relative humidity over the time course of the experiment. Cakes were removed from their original vial, placed on a glass slide and dispersed with silicon oil to isolate three different regions that were then covered with a glass coverslip and examined for crystallinity using a polarizing microscope (Olympus BX51) equipped with a 522 nm filter.

RESULTS

HPLC Analyses

Shown in Fig. 2 are HPLC chromatograms illustrating the baseline separation of Gly-Phe-L-Asn-Gly and its degradation products after storage of formulation A at 40°C/40% RH for 22.5 h (upper chromatogram), the same formulation at t_{zero} (middle chromatogram), and a blank formulation without Gly-Phe-L-Asn-Gly (lower chromatogram). A total of 10 degradants (i.e., D- and L-succinimides, D- and L-isoaspartates and aspartates, and four covalent Gly-Phe-L-Asn-Gly/Gly-Val adducts) could be monitored using this separation method. With the exception of the covalent adducts, identification of each peak was confirmed by comparing retention times against synthetic standards.

Separation of the D- and L-isoaspartates, aspartates, and succinimides from Gly-Phe-L-Asn-Gly was achieved in the isocratic mode by optimizing the pH of the buffered aqueous solvent system. At pH values near 4.1, Gly-Phe-L-Asn-Gly was relatively unaffected by changes in the mobile phase pH, allowing the selection of a pH where the more negatively charged isoaspartates eluted before Gly-Phe-L-Asn-Gly and the aspartates eluted after, due to their greater hydrophobicity (37). At a pH of 4.1, the isoaspartates elute first due to their greater negative charge. While both

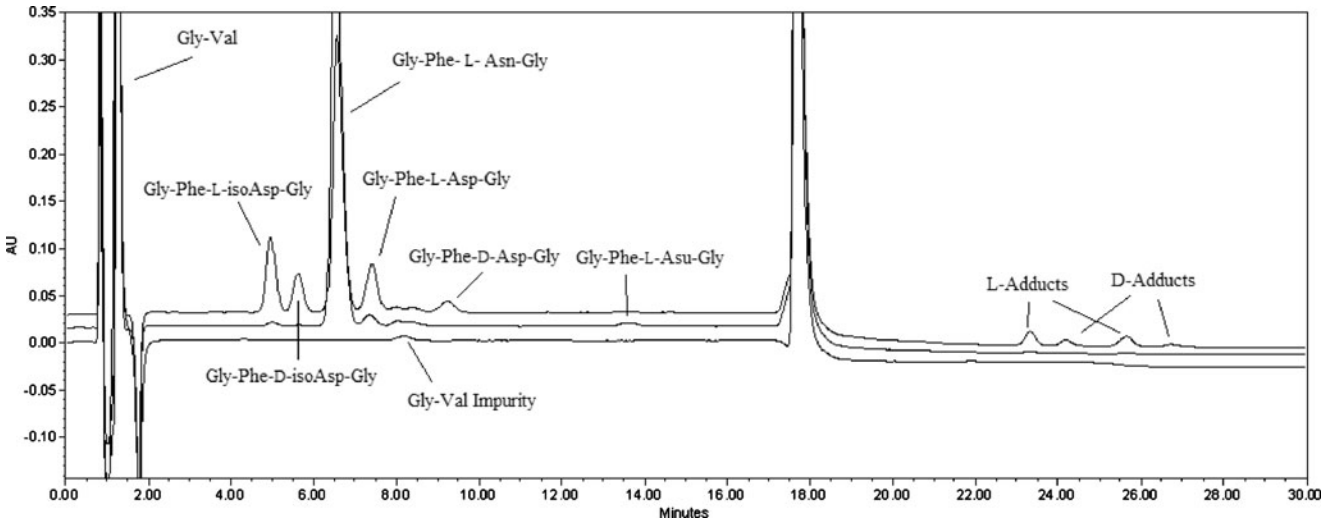

Fig. 2 Overlay of HPLC chromatograms generated at 220 nm. Peak at ~18 min was due to the step gradient at 16 min. Lower chromatogram: blank formulation without Gly-Phe-L-Asn-Gly. Middle chromatogram: Gly-Phe-L-Asn-Gly formulation A at t_{zero}. Upper chromatogram: Gly-Phe-L-Asn-Gly formulation A after storage for 22.5 h at 40°C and 40% relative humidity.

isoaspartates and aspartates have an additional ionizable –COOH, isoaspartates have a lower pKa compared to their aspartate counterparts (38). Using software from Advanced Chemistry Development, Inc., the pKa of the aspartyl α-COOH in Gly-Phe-isoAsp-Gly is predicted to be 2.96 compared to a value of 4.28 for the β-COOH in Gly-Phe-Asp-Gly. Thus, at pH 4.1, the β-COOH in aspartate-containing peptides is mostly protonated and the compounds are retained longer in reversed phase chromatography. Changes in pH had little effect on separation of the diastereomeric pairs (e.g., Gly-Phe-D-Asp-Gly and Gly-Phe-L-Asp-Gly). The chromatographic separation of the D- and L-succinimides is more clearly illustrated in Fig. 3.

As shown in Fig. 2, four peaks eluting at later retention times (23–27 min) were observed after lyophiles containing Gly-Phe-L-Asn-Gly were incubated at 40°C/40% RH for 22.5 h. These were identified (see below) as covalent adducts of Gly-Phe-L-Asn-Gly with Gly-Val. Achieving elution of the four covalent adduct peaks within a reasonable time frame required an increase in acetonitrile percentage from 0% to 5%, which could be accomplished using a step gradient at 16 min. The four adduct peaks were well resolved within a pH range of 3.9 to 4.2 while mobile phase pH values outside of this range resulted in partial co-elution of two or more peaks.

Covalent Adduct Characterization

The four unknown degradants having retention times between 23 and 27 min (Fig. 2) were postulated to be products of Gly-Val attack on L- and D-succinimide intermediates formed from Gly-Phe-L-Asn-Gly. To further test this hypothesis, lyophiles containing either the L- or D-succinimide (i.e., Gly-Phe-L-Asu-Gly or Gly-Phe-D-Asu-Gly) were prepared in the same formulation as that employed for the stability study of Gly-Phe-L-Asn-Gly in Fig. 2, stored for 2 h at 27°C and 75% RH, and monitored by HPLC. As shown in Fig. 3, the same degradant peaks observed in Fig. 2, apart from the succinimides themselves, were detected when the starting reactant was either the L- or D-succinimide. Breakdown of the L-succinimide (Fig. 3a) resulted in the formation of the two major hydrolysis products, Gly-Phe-L-Asp-Gly and Gly-Phe-L-isoAsp-Gly, and two major adduct peaks at relative retention times (RRT) of 3.6 and 3.9 (normalized to the retention time of Gly-Phe-L-Asn-Gly). Gly-Phe-D-Asp-Gly and Gly-Phe-D-isoAsp-Gly and two minor adduct peaks were also detected (Fig. 3a). Similarly, when the D-succinimide was incubated under the same conditions the major degradants were Gly-Phe-D-Asp-Gly and Gly-Phe-D-isoAsp-Gly with smaller amounts of their L-counterparts, along with two major adduct peaks with RRTs of 3.7 and 4.1 (Fig. 3b) and two minor adduct peaks. These results are consistent with partial racemization of the succinimides concurrent with hydrolysis and covalent adduct formation.

To tentatively assign a primary sequence to each adduct peak, fractions of the individual peaks were collected and analyzed by electrospray mass spectrometry. The mass spectrum of each HPLC peak indicated a molecular ion at m/z of 551 ($M+H^+$) consistent with the expected molecular weight for covalent adducts between Gly-Val and either an L- or D-succinimide. Fragmentation analysis by MS/MS (Fig. 4) indicated similar fragmentation patterns for the two peaks with RRTs of 3.6 and 4.1 (panels A and D) and similar patterns for the peaks with RRTs of 3.7 and 3.9 (panels B and C). The intensities of

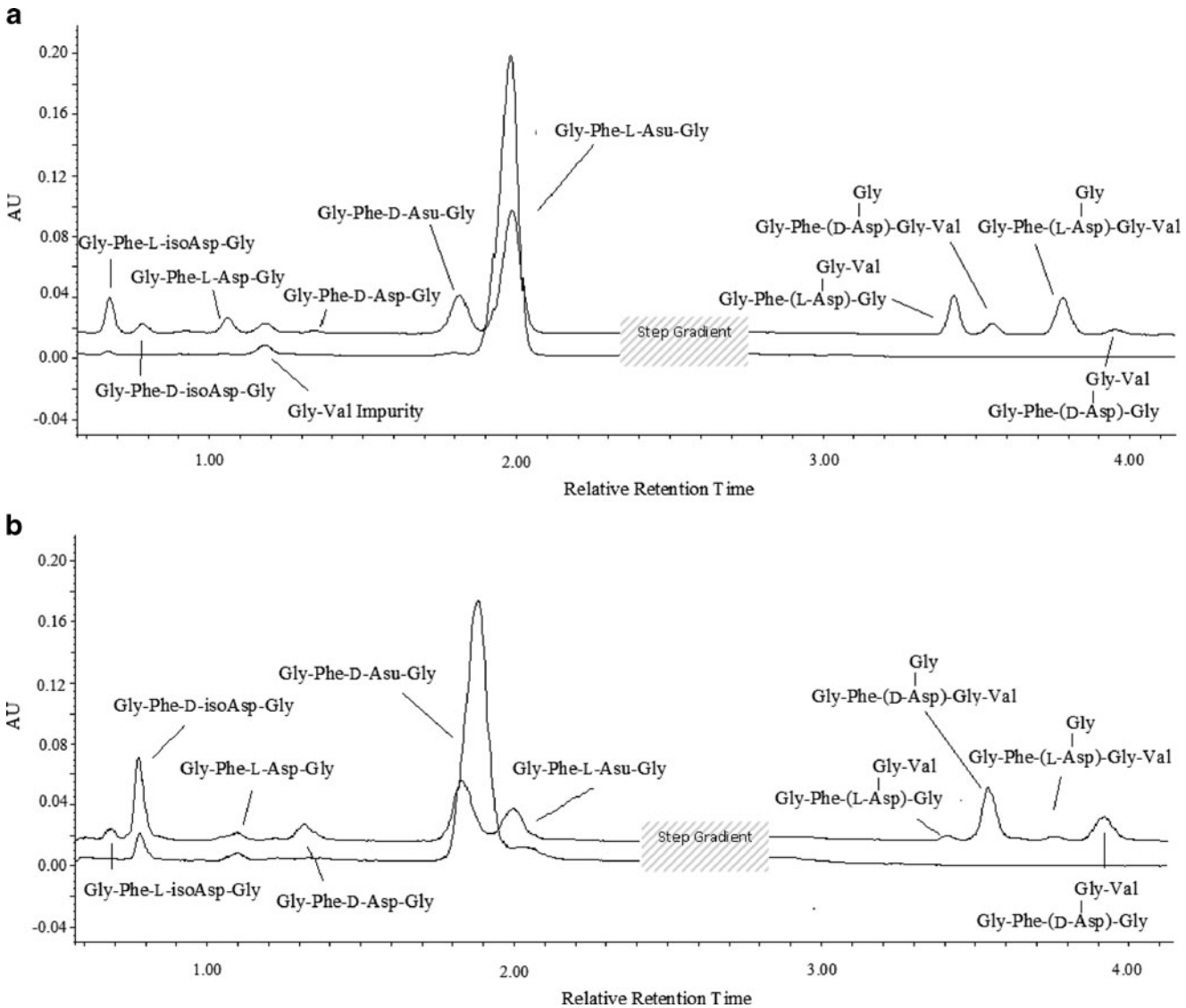

Fig. 3 Overlay of HPLC chromatograms showing the formation of degradants from the L-succinimide (**a**) and from the D-succinimides (**b**) after storage at 27°C and 75% RH for two hours. Lower chromatograms in each panel were generated post-lyophilization immediately prior to the kinetic studies. Disturbances in the chromatograms due to the step gradient were removed and baselines adjusted. Relative retention times reflect normalization of analyte retention times to that for Gly-Phe-L-Asn-Gly.

several peaks in the fragmentation pattern differ significantly between the two sets of spectra (e.g., 377 and 476 Da) and may offer insight as to the structure of each adduct. Lehmann *et al.* (39) assumed that fragmentation of peptides occurs primarily between the amide bonds of the peptide backbone, as facilitated by the formation of a five-membered oxazolone ring formed via intramolecular attack by the carbonyl oxygen on the N-terminal side of the peptide linkage undergoing cleavage. Incorporation of a methylene group into the peptide backbone in an isoaspartyl peptide hinders this fragmentation pathway as the intramolecular reaction would then involve formation of a less favored six-membered ring.

The above concept was applied to the MS/MS patterns from each covalent adduct peak in an attempt to obtain information pertaining to the primary sequence. Figure 5 illustrates the structures of the two adducts formed from Gly-Val attack at either the β-carbonyl (Fig. 5a) or the α-carbonyl (Fig. 5b) of Gly-Phe-L-Asu-Gly or Gly-Phe-D-Asu-Gly. As illustrated in Fig. 5a, intramolecular attack by the adjacent N-terminal side carbonyl oxygen would be expected to favor formation of a five-membered oxazolone ring fragment ($m/z = 476$ Da) over the six-membered ring ($m/z = 377$ Da), while in Fig. 5b, the same preference for a five-membered oxazolone ring would be expected to shift the ratio in favor of a fragment having a mass of 377 Da.

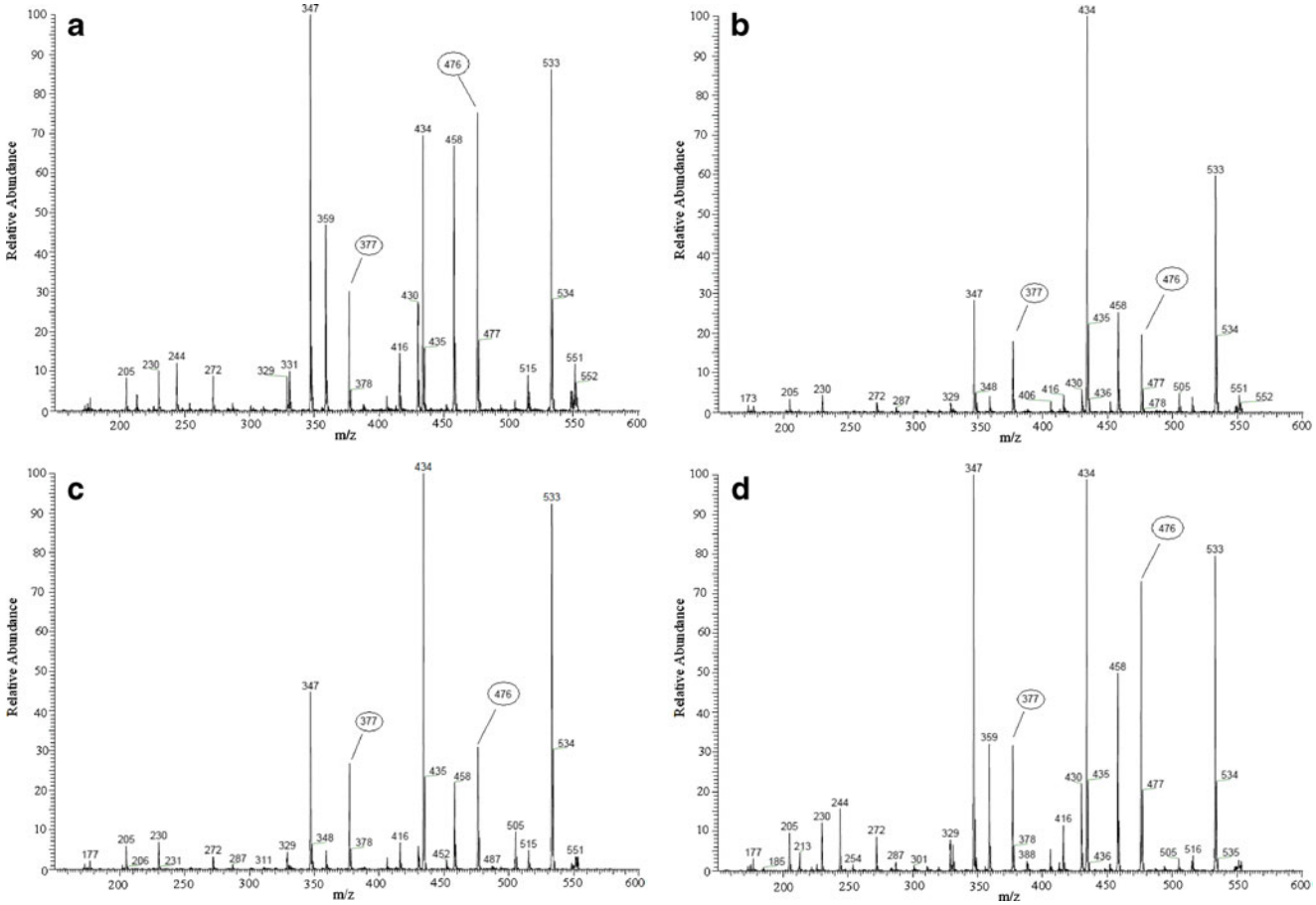

Fig. 4 MS/MS fragmentation patterns for the individual adduct peaks at RRT 3.6 (**a**), 3.7 (**b**), 3.9 (**c**), and 4.1 (**d**). Similar fragmentation patterns are observed between (**a**) and (**d**) and between (**b**) and (**c**). The fragmentation patterns suggest that the peptides at RRT 3.6 and 4.1 are structurally similar to each other and significantly different than the peptides at RRT 3.7 and 3.9. The tentative primary sequences assigned are listed in Table II.

An examination of panels A and D in Fig. 4 reveals a strong preference for the 476 Da fragment compared to the fragment at 377 Da, consistent with the above expectations, while the ratio of these peaks in panels B and C of approximately one indicates a distinct shift in favor of the 377 Da fragment. The 377 Da fragment reflecting loss of Gly-Val does not become dominant over the 476 Da fragment in panels B and C possibly due to other avenues for Gly removal in the adducts. This leaves some uncertainty in the structure assignments.

Combining the mass spectrometry data and HPLC degradation profiles for the L- and D-succinimides allowed each peak in Fig. 3 to be assigned a primary sequence. Accordingly, peaks with RRTs of 3.6 and 4.1 were tentatively assigned the sequence shown in Fig. 5a with the L-diastereomer eluting at a RRT of 3.6 and the D-diastereomer at RRT 4.1. The peaks with RRTs of 3.7 and 3.9 were then assigned the primary sequence in Fig. 5b with the D- and L-diastereomers eluting at 3.7 and 3.9, respectively. The structures assigned for all compounds of interest in this study are listed in Table II along with their relative retention times (RRT = 1.0 for Gly-Phe-L-Asn-Gly).

Determination of Relative Response Factors

The purity of each reference peptide was estimated based on the assumption that chromatographic molar response factors of each peptide are equal at 257 nm, as only the phenylalanine residue contributes to the UV absorbance at this wavelength. Consequently, the dipeptide Gly-Val does not exhibit a UV absorbance at 257 nm. To maximize the sensitivity of the HPLC assay for kinetic studies, a wavelength of 220 nm was selected. Relative response factors in relation to Gly-Phe-L-Asn-Gly for each peptide were therefore also determined at 220 nm taking into consideration the purity of each peptide. These results are shown in Table II along with the compound identities and relative retention times. Isoaspartate response factors were higher and those for aspartates were lower when compared to Gly-Phe-L-Asn-Gly which is consistent with previous reports in which response factors of Asn, Asp, and

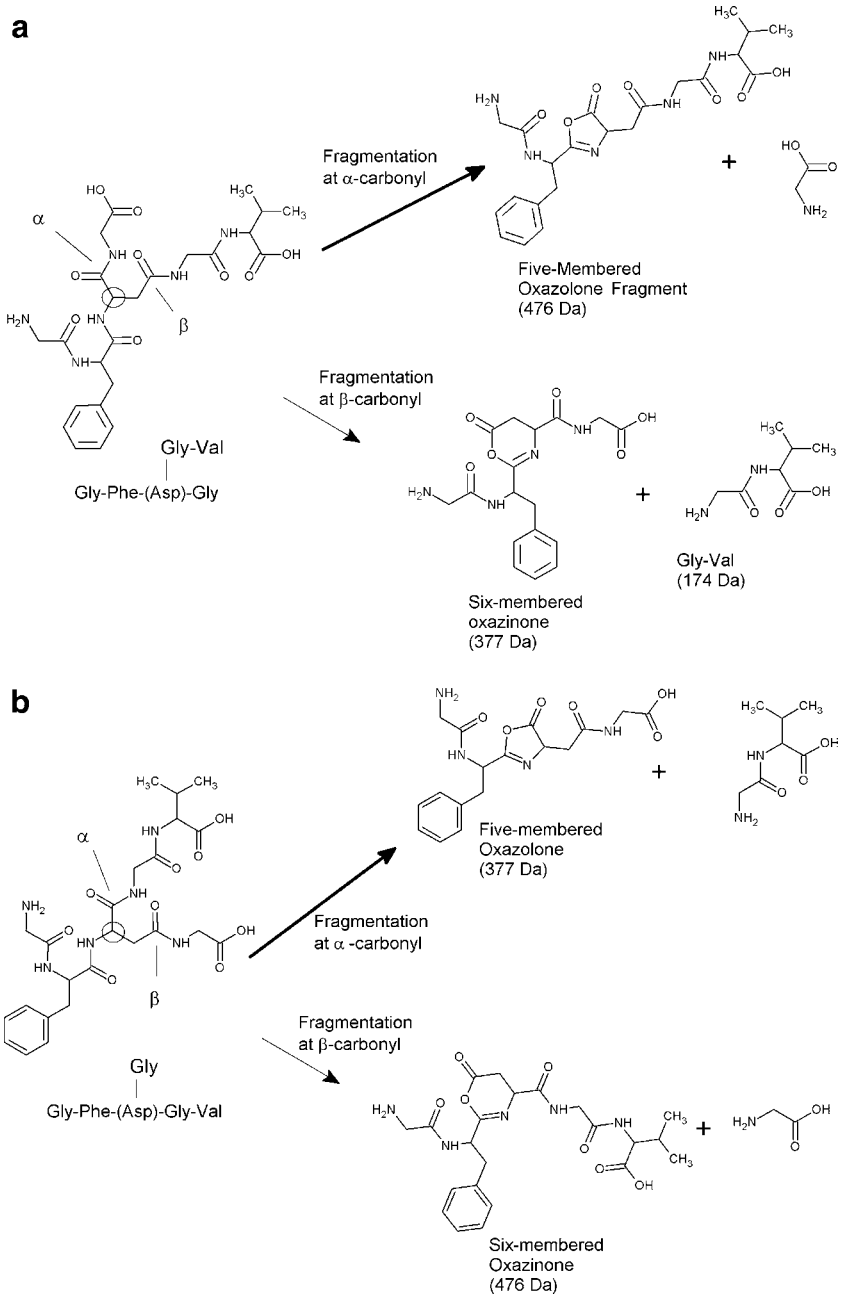

Fig. 5 Proposed structures (left) of the L- or D-adducts formed by attack of Gly-Val at the β- (**a**) or α- (**b**) carbonyls of the L- or D-succinimide intermediates (Gly-Phe-Asu-Gly). The chiral carbon where the changes in stereochemistry occur is circled. Labeled as α and β are points where peptide fragmentation may produce the fragments shown along with their molecular weights.

isoAsp-containing peptides have been compared (40). Generally, molar response factors at 220 nm increase with an increase in the number of peptide bonds contributing to the overall absorbance (41,42), accounting for the increase in response factors of the covalent adducts. The contribution of a succinimide residue to the response factor at 220 nm appears to be significantly higher than that of a normal peptide bond.

Characterization of Lyophiles Employed in Kinetic Experiments

Immediately after lyophilization, both formulations yielded white solid cakes occupying the same volume as the original solutions from which they were freeze-dried. After exposure to 40°C/40% RH for over 24 h formulation A samples were unchanged in appearance while formulation B lyophiles exhibited partial shrinkage to approximately 50% of their original fill height. The pH of reconstituted samples post lyophilization and at the end of kinetic experiments remained constant for both formulations. The average pH values for formulations A and B were 9.56 ± 0.01 and 9.60 ± 0.02, respectively. Polarized light microscopy indicated that samples of formulation A were completely amorphous and remained so after exposure to 40°C/40% RH. Slight evidence of birefringence was detected in formulation B lyophiles post-lyophilization,

Table II Relative HPLC Retention Times and Response Factors at 220 nm for the Ten Degradation Products Monitored in Degraded Formulations of Gly-Phe-L-Asn-Gly. Retention Times and Response Factors were Normalized to Those for Gly-Phe-L-Asn-Gly, Which Exhibited a Retention Time of 6.75 min

Peptide	Relative Retention Time	Relative Response Factor @ 220 nm
Gly-Phe-L-Asn-Gly (RT = 6.75 min)	1.0	1.00
Gly-Phe-L-isoAsp-Gly	0.77	1.15
Gly-Phe-D-isoAsp-Gly	0.87	1.17
Gly-Phe-L-Asp-Gly	1.1	0.871
Gly-Phe-D-Asp-Gly	1.4	0.794
Gly-Phe-D-Asu-Gly	2.0	1.47
Gly-Phe-L-Asu-Gly	2.1	
Gly-Val | Gly-Phe-(L-Asp)-Gly	3.6	1.39
Gly | Gly-Phe-(D-Asp)-Gly-Val	3.7	
Gly | Gly-Phe-(L-Asp)-Gly-Val	3.9	
Gly-Val | Gly-Phe-(D-Asp)-Gly	4.1	

which became increasingly apparent after storage at 40°C/40% RH (results not shown). This was attributed to partial crystallization of Gly-Val that continued to increase with time. Moisture contents in lyophiles were determined by the Karl-Fischer titration method. Inorganic oxides, including carbonate, are known to contribute a stoichiometric amount of water to the apparent water content determination by Karl-Fischer titrations (43). This was verified in our studies by comparing the apparent water content in vacuum dried Gly-Val/carbonate lyophiles varying in carbonate content with lyophiles containing only Gly-Val. The contribution of carbonate buffer was therefore subtracted from the apparent water content determined for formulation A. After equilibration at 40% RH, water content was very similar for both formulations (16.9± 1.6% in formulation A and 14.0±1.7%, in formulation B) and was unchanged at the end of the kinetic studies. Based on these results, the most significant difference between the two formulations was the partial crystallization of Gly-Val in formulations containing higher concentrations of Gly-Val. The theoretical compositions of each lyophile are summarized as weight percentages in Table I (after equilibration at 40% RH).

Kinetics of Gly-Phe-L-Asn-Gly Deamidation and Degradant Formation

Lyophile formulations A and B were stored at 40°C/40% RH and reconstituted to their original solution volume at various times for HPLC analysis. The concentration over time for the duplicate preparations of formulation A is shown in Fig. 6a,c. The concentration of the adducts and hydrolysis degradants, along with Gly-Phe-L-Asn-Gly, are almost identical. This indicates that the variability between formulations in the total amount of adduct or aspartates formed is minimal. However, there is some observable variability in the succinimide concentration over time which directly correlates to larger confidence intervals in the calculated rate constant. The average confidence limit for formulation A prepared in duplicate is approximately 29% of the calculated value compared to 22% for the single preparation of formulation B. Therefore, the precision of the calculated rate constants showed no improvement for formulations prepared in duplicate.

Shown in Fig. 6a,b are the Gly-Phe-L-Asn-Gly and degradant concentrations in the two formulations plotted *versus* time on a semi-log scale. The degradant concen-

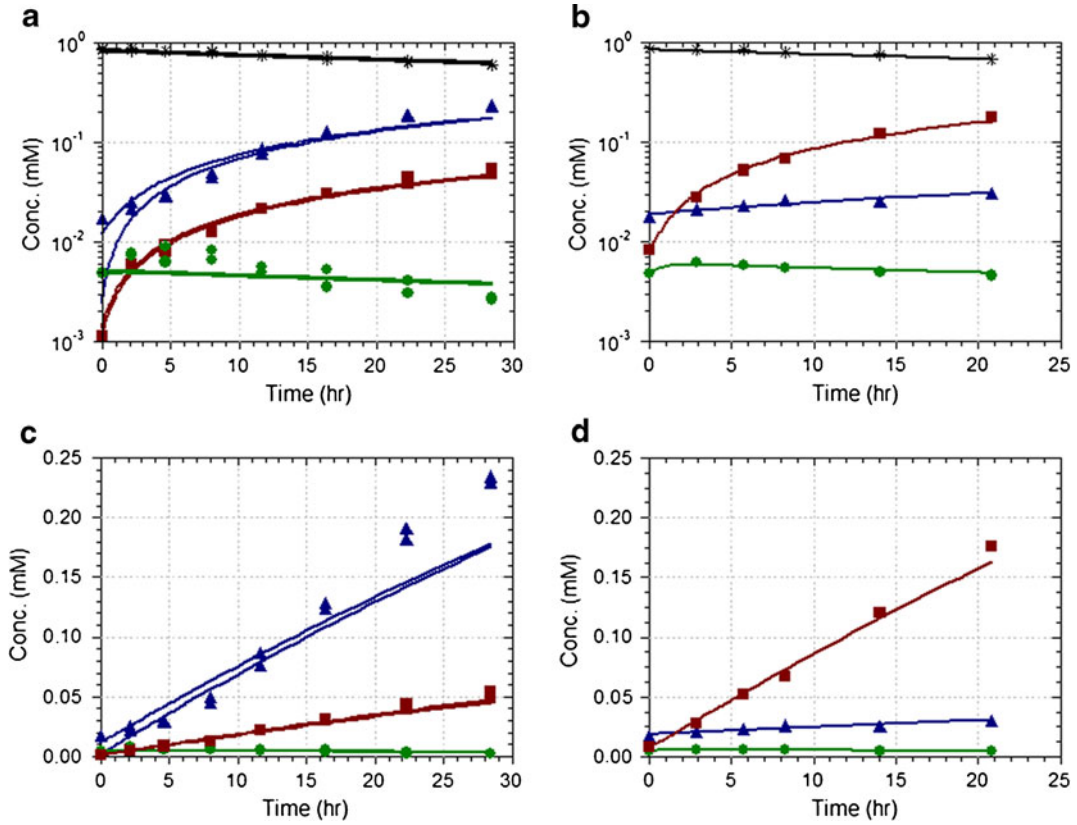

Fig. 6 Concentrations of Gly-Phe-L-Asn-Gly (*), succinimide (●), L- and D-aspartate and isoaspartate hydrolysis products (▲) and L- and D-covalent adducts (■) in lyophile formulations as a function of time at 40°C/40% RH. Concentrations in lyophiles of formulation A prepared in duplicate and single preparation of formulation B are displayed semilogarithmically in (**a**) and (**b**), respectively. Shown in (**c**) and (**d**) are the degradant concentrations from formulations A (in duplicate) and B (single), respectively, on a linear scale.

trations are shown on a linear scale in Fig. 6c,d. For clarity and to illustrate the competition between hydrolysis and covalent adduct formation, the D- and L-isoaspartate and aspartate concentrations were combined and represented in Fig. 6 as "aspartates" while the four covalent adducts were summed together and displayed as "adducts". These degradants accounted for the bulk of the products formed from the degradation of Gly-Phe-L-Asn-Gly over the first ~25% decomposition as supported by the finding that the mass balances within this window were >95%.

As evident in Fig. 6, the succinimide concentrations in either formulation remained at a steady-state concentration of ~1% of the starting peptide concentration throughout the experiments, indicating that the succinimide is a reactive intermediate and that its formation is rate-determining. Aspartates were the dominant products formed in formulation A (Fig. 6c), in which the Gly-Val concentration was present at an ~8-fold molar excess over Gly-Phe-L-Asn-Gly, while in formulation B containing a ~30-fold molar excess of Gly-Val, covalent adduct formation dominated (Fig. 6d).

Differential equations based on Fig. 1 were used to simultaneously fit the Gly-Phe-L-Asn-Gly, succinimide, aspartates and covalent adduct concentrations *versus* time as illustrated by solid lines in Fig. 6. The excellent fits provide support for the applicability of the reaction pathways described in Fig. 1 to the degradation of Gly-Phe-L-Asn-Gly in these solid-state lyophile formulations. Pseudo-first order rate constants for the disappearance of Gly-Phe-L-Asn-Gly and the formation of aspartates and adducts were calculated based on Fig. 1 as summarized in Table III. The estimated rate constants for succinimide formation ($0.01\ h^{-1}$) were not significantly different in the two formulations and the overall rate of breakdown of the succinimide also did not differ significantly. However, the rate constants for succinimide hydrolysis and covalent adduct formation were highly sensitive to formulation. In formulation B where the Gly-Val concentration was far in excess (i.e., 30-fold) of the Gly-Phe-L-Asn-Gly concentration, the rate constant for covalent adduct formation exceeded that for imide hydrolysis by >10-fold when both were expressed in first-order units. In contrast, the lower

Table III Rate Constants for the Parameters Described in Eqs. 1–4 and Fig. 1 Generated from Kinetic Studies of Lyophilized Formulations A and B at 40°C/40% RH. Rate Constants were Assumed to be First-Order or Pseudo-First Order with Units of hr^{-1}. For Covalent Adduct Formation, 2nd Order Rate Constants were also Generated by Dividing First-Order Rate Constants by the Calculated Molar Concentrations of Gly-Val in the Two Formulations (Table II). 95% Confidence Intervals are Reported in Parentheses

Parameter	Pseudo-first order rate constants (hr^{-1})		Second order rate constants (M^{-1} h^{-1})	
	Formulation A[a]	Formulation B	Formulation A	Formulation B
k_{imide} (Gly-Phe-L-Asn-Gly→Imide)	0.0104 (0.008–0.013)	0.0106 (0.009–0.0119)	–	–
$k_{aspartates}$ (Imide→Aspartates)	1.35 (0.95–1.76)	0.109 (0.065–0.152)	–	–
k_{adduct} (Imide→Adducts)	0.36 (0.25–0.47)	1.38 (1.20–1.57)	0.49 (0.34–0.65)	0.47 (0.41–0.54)

[a] rate constants represent the calculated value from the simultaneous fit of duplicate formulations

Gly-Val concentration in formulation A resulted in a commensurate reduction in the rate constant for covalent adduct formation. This can be rationalized by considering the dilution effect expected for a bimolecular reaction as illustrated by Eq. 5.

$$\frac{d[Adduct]}{dt} = k'_{adduct}[GlyVal][Imide] \quad (5)$$

When the differences in Gly-Val concentration were taken into account by calculating 2nd order rate constants for covalent adduct formation, the bimolecular rate constants were similar, suggesting that covalent adduct formation is first-order in the solid-state concentration of Gly-Val. The pseudo first-order rate constant for succinimide hydrolysis increased significantly in formulation A compared to formulation B, despite the fact that the water content in the two lyophiles was similar.

DISCUSSION

Deamidation Pathway in Amorphous Lyophiles

Although quantitative differences have been noted, most mechanistic comparisons of the pathways for deamidation of asparagine-containing peptides in aqueous solutions and amorphous solids have concluded that deamidation proceeds through a succinimide intermediate in both cases except perhaps at low pH. In aqueous solutions from approximately pH 5–12, cyclic imide intermediate (16,44) formation is the rate-determining step and leads to a mixture of L- and D-aspartyl peptides and isoaspartyl peptides (15). Primary structure is very important in determining the rates of succinimide formation with reactions at X–Asn-Gly- sequences being particularly favorable (15,45). Ratios of isoaspartyl/aspartyl hydrolysis products in aqueous solution typically range from 3:1 to 4:1, reflecting more favorable water attack at the α-carbonyl of the succinimide. Geiger and Clarke, for example, found that deamidation of a model hexapeptide Val-Tyr-Pro-L-Asn-Gly-Ala at pH 7.4 and 37°C produced approximately 71% L-hydrolysis products with an isoaspartyl/aspartyl ratio of 3.6 and 29% D-hydrolysis products with an isoaspartyl/aspartyl ratio of 3.1. Patel and Borchardt explored the pH dependence for deamidation of the same hexapeptide from pH 5–12 in various buffers and obtained isoaspartyl/aspartyl peptide ratios that were nearly constant with pH, ranging from ~3.5 at pH 6 to 4.2 at pH 12 and comparable to the ratios obtained when using the cyclic imide as the starting reactant (44). The detection of isoaspartyl peptides is often taken as evidence for the involvement of a succinimide intermediate, as this is the only known pathway leading to these products. Moreover, the nearly identical isoaspartyl/aspartyl product ratios found by Patel and Borchardt when starting with either the Asn-containing peptide or the succinimide suggests that deamidation proceeded entirely via this intermediate under the conditions employed in that study. The extent to which racemization in aqueous solutions is mediated by the cyclic imide, as originally proposed by Geiger and Clarke (15), is less clear. Li *et al.* (23) found partial racemization of Gly-Gln-L-Asn-Glu-Gly (GQ-L-Asn-EG) to GQ-D-Asn-EG and *vice versa* during deamidation at pH 10 and 70°C, which they attributed to tetrahedral intermediate involvement in the racemization. Regardless, there is no dispute that racemization occurs along the cyclic-imide-mediated reaction pathway ultimately leading to deamidation.

Lai and Topp (3) noted that the mechanisms for peptide deamidation in amorphous lyophiles appear to be similar to those in solution but with some significant quantitative differences. For example, Oliyai *et al.* (46) detected cyclic imide formation in amorphous solids during deamidation of the same hexapeptide originally explored by Geiger & Clarke, but were unable to find the isoaspartyl hydrolysis product. Lai *et al.* (47) examined the stability of this hexapeptide in poly(vinyl alcohol) and poly(vinyl pyrrolidone) (PVP) glassy state formulations and were able to detect the isoaspartyl hydrolysis product as one of the dominant degradants along with the succinimide, again consistent with a cyclic imide mediated pathway. Song *et al.*

(48) monitored the same reaction in PVP as a function of effective 'pH' in both glassy and rubbery states, defined as the pH measured in aqueous solution either prior to lyophilization or after reconstitution. At 'pH' >5 and 70°C, the isoaspartyl/aspartyl deamidated product ratios were in the range of 3.0–5.0 in rubbery PVP solids, glassy PVP solids, and in solution, again suggesting that cyclic imide formation plays a central role in the deamidation of this peptide in both solution and amorphous solid formulations.

As demonstrated in Fig. 2, the degradation of Gly-Phe-L-Asn-Gly in amorphous lyophiles resulted in the formation of both L- and D-succinimides as well as the L- and D-isoaspartyl and aspartyl hydrolysis products (i.e., four hydrolysis products). Plots in Fig. 6 for the formation of aspartates from Gly-Phe-L-Asn-Gly in amorphous lyophiles stored at 40°C/40% RH could be fit by the model described in Fig. 1, which assumes that aspartates form via a cyclic imide intermediate. While isoaspartyl/aspartyl product formation rates were not a focal point of this study, a more detailed kinetic model that includes all degradant species is being developed (to be published). Preliminary results indicate that the isoaspartyl to aspartyl formation rate constant ratios in amorphous lyophiles under the conditions described herein are 2.6 and 2.2, respectively, from the L- or D-succinimide. Both primary sequence in peptides (49) and the local microenvironment resulting from the three-dimensional structure in proteins (21) can influence the ratios of products formed from deamidation. Likewise, the local microenvironment within amorphous lyophiles may also influence this ratio. The finding that the same four hydrolysis products are formed in approximately the same ratios when starting from either the intact L-Asn containing tetrapeptide or its corresponding L-succinimide, combined with the excellent fits of the data obtained when applying the model in Fig. 1 to fit the concentration *versus* time data in Fig. 6, establish that the deamidation of the tetrapeptide occurs via a succinimide mediated mechanism in the amorphous solid formulations explored herein.

Covalent Adduct Formation between Gly-Phe-L-Asn-Gly and Gly-Val in Amorphous Lyophiles

Our own previous finding that deamidation at the A-21 asparagine residue in insulin is accompanied by covalent amide-linked dimer formation and that both the aspartate hydrolysis product and covalent dimers form via a highly reactive cyclic anhydride intermediate (25–30) led to the hypothesis that similar opportunities for covalent, amide-linked aggregate formation may be available for reactions that involve reactive cyclic imide intermediates, even though cyclic imides are less reactive than cyclic anhydrides. Given this possibility, it is curious that there are few reports in the literature outside of those pertaining to insulin in which amide-linked covalent aggregates have been identified. Some reports of non-reducible aggregate formation have considered the possibility for succinimide intermediate involvement, as summarized below, but have offered no mechanistic proof.

Paranandi *et al.* (50) reported that deamidation of synapsin leading to isoaspartate formation in pH 7.4 buffers at 37°C was accompanied by intermolecular cross-linking reactions to produce both reducible, disulfide linked aggregates as well as non-reducible, irreversible aggregates. The authors speculated that the non-reducible aggregates may have been due to lysinoalanine cross-linking to dehydroalanine formed by via β-elimination in cystine residues but they also offered another possibility—that the covalent aggregate formation may have been linked to isoaspartate formation. Thus, they postulated that intermolecular nucleophilic attack by the ε-amino group of a lysine residue in one synapsin molecule at either the α- or β-carbonyl of a succinimide intermediate on a second synapsin molecule could be the source of the non-disulfide linked aggregates.

Stabilization of phage capsid proteins such as phage HK97 occurs through covalent amide cross-linking between lysine residues and Asn^{356} side-chains of adjacent subunits. Such cross-links may be widespread in gram-positive bacteria (51). Wikoff *et al.* (52) suggested that this reaction may be mediated through cyclic imide formation from asparagines followed by nucleophilic attack by lysine. Glu^{363} is a critical catalyst for this reaction, which the authors suggested may increase the nucleophilicity of the backbone amide nitrogen of the Asn^{356}. However, Dierkes *et al.* (53) advocated an alternative mechanism involving direct Glu^{363} assisted lysine attack on the amide side-chain of Asn^{356} because they were unable to find any compelling evidence for the presence of succinimide.

In 2002, Simons *et al.* (54) demonstrated that storage of lyophiles produced from a pH 7 solution of RNase A under vacuum at 85°C for successive 24 h periods resulted in the formation of covalent cross-linking to form dimers, trimers, and tetramers. This "zero-length" cross linking was attributed to the formation of intermolecular amide bonds between residues on different RNase molecules that were located in close proximity to each other in the lyophiles. The yield of covalent dimers was approximately 30% but in the presence of increasing ratios of the excipient trehalose, dimer formation was reduced dramatically. Despite the known involvement of Asn and Gln deamidation in the instability of RNase A at pH 7, (5) cyclic imide involvement was not considered. Maroufi *et al.* (55) later employed the same method to produce an amide-linked dimer of hen egg-white lysozyme.

The recent observation of a linear relationship between the quantity of dimers formed and the% of succinimide in freeze-

dried lysozyme powder stored for up to 7 days at 80°C (34) is the most definitive evidence we had seen, prior to our own work, suggesting a role for this intermediate in covalent aggregate formation. The formation of covalent adducts in amorphous lyophiles of Gly-Phe-L-Asn-Gly in the presence of excess quantitites of Gly-Val found in the present study directly demonstrates that succinimide formation can lead to nonreducible, covalent amide-linked peptide aggregates.

As illustrated in Fig. 2, in addition to the normally expected degradants produced by succinimide formation, racemization, and hydrolysis, four covalent adducts were also observed during storage of amorphous lyophiles of Gly-Phe-L-Asn-Gly in the presence of excess Gly-Val under accelerated storage conditions (40°C and 40% RH). Each adduct exhibited a molecular ion ($(M+H)^+$ = 551 Da) by electrospray mass spectrometry consistent with the combination of Gly-Phe-L-Asn-Gly and Gly-Val (minus a molecule of water). Tandem MS/MS analysis (Figs. 4 and 5) also indicated fragmentation patterns consistent with Gly-Val attack at either the α- or β-carbonyls of Gly-Phe-L-Asu-Gly or Gly-Phe-D-Asu-Gly. These fragmentation patterns, along with the results in Fig. 3 showing that adduct peaks 1 and 3 originate from Gly-Phe-L-Asu-Gly and adduct peaks 2 and 4 predominate when Gly-Phe-D-Asu-Gly is the initial reactant, enabled us to tentatively assign the structures indicated in Fig. 2 and Table II. The number of adducts was limited to just four by the use of an excess of Gly-Val, which minimized the extent to which Gly-Phe-L-Asn-Gly dimers, trimers, etc. could form.

Under the experimental conditions described, covalent adducts form exclusively through the succinimide intermediates generated during deamidation of asparagines as supported by the following observations: 1) The same products, including adducts, are produced when the initial reactant is Gly-Phe-L-Asn-Gly, Gly-Phe-L-Asu-Gly; or Gly-Phe-D-Asu-Gly; and 2) the kinetic model in Fig. 1 is successful in simultaneously fitting concentration *vs.* time data in Fig. 6 for the disappearance of Gly-Phe-L-Asn-Gly, succinimide intermediates, isoaspartate and aspartate hydrolysis products resulting from succinimide hydrolysis, and covalent adducts forming from reaction of the succinimide with Gly-Val in two formulations varying in the amount of excess Gly-Val.

Kinetics and Succinimide Intermediate Partitioning to Hydrolysis Products or Covalent Adducts—Effect of Gly-Val Dilution in Lyophiles

The complexity and multi-step nature of the reactions involved in peptide deamidation and covalent adduct formation, even when using a simplified model such as that depicted in Fig. 1, suggests that attempts to interpret reaction rates or relative amounts of degradant production based solely on the notion that reactivity should be coupled to mobility as measured by various structural relaxation parameters (56) may fall short of expectations. A detailed examination of the parameter values generated from the application of the model in Fig. 1 to the kinetic data in Fig. 6, as listed in Table III, suggests that attempts to rationalize changes in reactivity in amorphous solids in terms of a coupling constant to molecular mobility should consider each reaction step separately as well as the nature of each step. In the two formulations being compared, the rate constants for rate-determining formation of succinimide did not differ significantly, despite the fact that partial collapse and partial crystallization of Gly-Val in lyophile formulation B were observed after exposure to 40% RH while no changes were detected in formulation A, suggesting greater structural relaxation and mobility in formulation B. Given that succinimide formation is an intramolecular reaction involving only local conformational changes (although ammonia diffusion away from the reaction site must ultimately occur), perhaps it would not be surprising that motions governing structural relaxation may not be relevant. It is more likely that a bimolecular reaction, such as the attack of Gly-Val on the succinimide, would exhibit a greater degree of coupling to mobility. However, the differences in apparent first-order rate constants for covalent adduct formation could be adequately accounted for by a dilution effect (Eq. 5 and Table III), without regard to mobility.

Amorphous lyophile formulations differ from aqueous solutions both in terms of reactant mobility but also with respect to their chemical microenvironment (i.e., proteins and excipients employed in such products would create a solvent environment most closely resembling polar organic solvents). Severs & Froland recently explored organic solvents to stabilize a 31 amino acid containing polypeptide that underwent deamidation in aqueous solution at two Asn residues, with the expectation that stability in an organic solvent would be superior (57). Instead, in DMSO they observed the formation of multiple covalent dimers and higher order multimers. The hypothesis advanced by the authors was that cyclic imides could form from either the two Asn or two Asp residues in the molecule followed by nucleophilic attack by one of nine possible nucleophiles (including lysine, serine, and threonine residues), thus generating a large number of reaction products, including dimers, polymers, cyclic imides, and conformational isomers.

Possibly, covalent aggregates are seldom detected or identified in Asn-containing peptide and protein lyophiles during long-term storage because the population of covalent aggregates generated may be widely distributed among numerous reaction products.

CONCLUSION

Kinetic studies of the decomposition of a model asparagine-containing peptide in amorphous lyophile formulations in the presence of an excess of a second peptide (Gly-Val) demonstrated that deamidation and racemization proceed through a succinimide intermediate. Moreover, a total of ten degradants were monitored, four of which were characterized as covalent adducts resulting from the attack of Gly-Val on the D- and L-succinimide intermediates. The same degradant profiles were found in lyophile formulations containing the succinimide as the starting reactant. A model based on the assumption that the succinimide lies on the reaction pathway for formation of all degradants was quantitatively consistent with the kinetic data. The reaction pathways presented in this study suggest a potentially important mechanism for the formation of non-reducible, covalent aggregates in lyophilized protein and peptide formulations. While factors that affect molecular mobility (e.g., excipients, water content, etc.) clearly need to be considered in predicting or at least rationalization reaction rates and degradant profiles in solid-state formulations, the observations herein highlight the importance of the underlying chemistry and the complexity of drug degradation processes in solid-state formulations, most of which involve one or more reactive intermediates and multiple reaction steps that may vary in reaction order.

ACKNOWLEDGMENTS & DISCLOSURES

The authors thank the faculty at the University of Kentucky Mass Spectrometry Facility for generating the mass spectra and for their helpful discussions. Partial support for this project was provided by the H.B. Kostenbauder Endowed Professorship.

REFERENCES

1. Manning MC, Patel K, Borchardt RT. Stability of protein pharmaceuticals. Pharm Res. 1989;6(11):903–18.
2. Schoneich C, Hageman MJ, Borchardt RT. Stability of peptides and proteins. In: Park K, editor. Controlled drug delivery challenges and strategies. Washington: American Chemical Society; 1997. p. 205–28.
3. Lai MC, Topp EM. Solid-state chemical stability of proteins and peptides. J Pharm Sci. 1999;88:489–500.
4. Manning MC, Chou DK, Murphy BM, Payne RW, Katayama DS. Stability of protein pharmaceuticals: an update. Pharm Res. 2010;27:544–75.
5. Zale SE, Klibanov AM. Why does ribonuclease irreversibly inactivate at high temperatures? Biochemistry. 1986;25:5432–44.
6. Costantino HR, Langer R, Klibanov AM. Solid-phase aggregation of proteins under pharmaceutically relevant conditions. J Pharm Sci. 1994;83(12):1662–9.
7. Nguyen TH. Oxidation degradation of protein pharmaceuticals. In: Cleland JL, Langer R, editors. Formulation and delivery of proteins and peptides. Washington: American Chemical Society; 1994. p. 59–71.
8. Griffiths SW, King J, Cooney CL. The reactivity and oxidation pathway of cysteine 232 in recombinant human α1-antitrypsin. J Biol Chem. 2002;277:25486–92.
9. Griffiths SW, Cooney CL. Development of a peptide mapping procedure to identify and quantify methionine oxidation in recombinant human a1-antitrypsin. J Chrom A. 2002;942:133–43.
10. Volkin DB, Klibanov AM. Thermal destruction processes in proteins involving cystine residues. J Biol Chem. 1987;262(7):2945–50.
11. Wu S-L, Leung D, Tretyakov L, Hu J, Guzzetta A, Wang YJ. The formation and mechanism of multimerization in a freeze-dried peptide. Int J Pharm. 2000;200:1–16.
12. Aswad DW. Deamidation and isoaspartate formation in peptides and proteins. Boca Raton: CRC Press; 1995.
13. Robinson NE, Robinson AB. Molecular clocks—Deamidation of asparaginyl and glutaminyl residues in peptides and proteins. Cave Junction: Althouse; 2004.
14. Wright HT. Nonenzymatic deamidation of asparaginyl and glutaminyl residues in proteins. Crit Rev Biochem Mol Biol. 1991;26:1–52.
15. Geiger T, Clarke S. Deamidation, isomerization, and racemization at asparaginyl and aspartyl residues in peptides. Succinimide-linked reactions that contribute to protein degradation. J Biol Chem. 1987;262:785–94.
16. Clarke S, Stephenson RS, Lowenson JD. Lability of asparagine and aspartic acid residues in proteins and peptides: Spontaneous deamidation and isomerization reactions. In: Ahern TJ, Manning MC, editors. Stability of Protein Pharmaceuticals Part A. New York: Plenum Press; 1992. p. 1–30.
17. Capasso S, Mazzarella L, Sica F, Zagon A. Deamidation via cyclic imide in asparaginyl peptides. Peptide Res. 1989;2:195–200.
18. Brennan TV, Clarke S. Spontaneous degradation of polypeptides at aspartyl and asparaginyl residues: effects of the solvent dielectric. Protein Sci. 1993;2(3):331–8.
19. Konuklar FAS, Aviyente V. Modelling the hydrolysis of succinimide: formation of aspartate and reversible isomerization of aspartic acid via succinimide. Org Biomol Chem. 2003;1(13):2290–7.
20. Brennan TV, Clarke S. Deamidation and iso-aspartate formation in model synthetic peptides: the effects of sequence and solution environment. In: Aswad DS, editor. Deamidation and iso-aspartate formation in peptides and proteins. Ann Arbor: CRC Press; 1995. p. 65–90.
21. Athmer L, Kindrachuk J, Georges F, Napper S. The influence of protein structure on the products emerging from succinimide hydrolysis. J Biol Chem. 2002;277(34):30502–7.
22. Capasso S, Di Cerbo P. Kinetic and thermodynamic control of the relative yield of the deamidation of asparagine and isomerization of aspartic acid residues. J Pept Res. 2000;56(6):382–7.
23. Li B, Borchardt RT, Topp EM, VanderVelde D, Schowen RL. Racemization of an asparagine residue during peptide deamidation. J Am Chem Soc. 2003;125(38):11486–7.
24. Dehart MP, Anderson BD. The role of the cyclic imide in alternate degradation pathways for asparagine-containing peptides and proteins. J Pharm Sci. 2007;96(10):2667–85.
25. Darrington RT, Anderson BD. The role of intramolecular nucleophilic catalysis and the effects of self-association on the deamidation of human insulin at low pH. Pharm Res. 1994;11:784–93.
26. Darrington RT, Anderson BD. Evidence for a common intermediate in insulin deamidation and covalent dimer formation: effects

of pH and aniline trapping in dilute acidic solutions. J Pharm Sci. 1995;84:275–82.
27. Darrington RT, Anderson BD. Effects of insulin concentration and self-association on the partitioning of its A-21 cyclic anhydride intermediate to desamido insulin and covalent dimer. Pharm Res. 1995;12:1077–84.
28. Strickley RG, Anderson BD. Mechanism of degradation of human insulin in solution and solid-state between pH 2–5. Pharm Res. 1994;11(10):S-72.
29. Strickley RG, Anderson BD. Solid-state stability of human insulin I. Mechanism and the effect of water on the kinetics of degradation in lyophiles from pH 2–5 solutions. Pharm Res. 1996;13:1142–53.
30. Strickley RG, Anderson BD. Solid-state stability of human insulin II. Effect of water on reactive intermediate partitioning in lyophiles from pH 2–5 solutions—stabilization against covalent dimer formation. J Pharm Sci. 1997;86:645–53.
31. Li B, Gorman EM, Moore KD, Williams T, Schowen RL, Topp EM, *et al.* Effects of acidic N + 1 residues on asparagine deamidation rates in solution and in the solid state. J Pharm Sci. 2005;94(3):666–75.
32. Li B, O'Meara MH, Lubach JW, Schowen RL, Topp EM, Munson EJ, *et al.* Effects of sucrose and mannitol on asparagine deamidation rates of model peptides in solution and in the solid state. J Pharm Sci. 2005;94:1723–35.
33. Li B, Schowen RL, Topp EM, Borchardt RT. Effect of N-1 and N-2 residues on peptide deamidation rate in solution and solid state. AAPS J. 2006;8(1):E166–73.
34. Desfougeres Y, Jardin J, Lechevalier V, Pezennec S, Nau F. Succinimidyl residue formation in hen egg-white lysozyme favors the formation of intermolecular covalent bonds without affecting its tertiary structure. Biomacromolecules. 2011;12:156–66.
35. Conrad U, Fahr A, Scriba GKE. Kinetics of aspartic acid isomerization and enantiomerization in model aspartyl tripeptides under forced conditions. J Pharm Sci. 2010;99:4162–73.
36. Schon I, Kisfaludy L. Formation of aminosuccinyl peptides during acidolytic deprotection followed by their transformation to piperazine-2,5-dione derivatives in neutral media. Int J Pept Protein Res. 1979;14:485–95.
37. Sereda TJ, Mant CT, Sönnichsen FD, Hodges RS. Reversed-phase chromatography of synthetic amphipathic α-helical peptides as a model for ligand/receptor interactions. Effect of changing hydrophobic environment on the relative hydrophilicity/hydrophobicity of amino acid side-chains. J Chromatogr, A. 1994;676:139–53.
38. Capasso S. Thermodynamic parameters of the reversible isomerization of aspartic residues via a succinimide derivative. Thermochim Acta. 1996;286(1):41–50.
39. Lehmann WD, Schlosser A, Erben G, Pipkorn R, Bossemeyer D, Kinzel V. Analysis of isoaspartate in peptides by electrospray tandem mass spectrometry. Protein Sci. 2000;9 (11):2260–8.
40. Stevenson CL, Anderegg RJ, Borchardt RT. Comparison of separation and detection techniques for human growth hormone releasing factor (hGRF) and the products derived from deamidation. J Pharm Biomed Anal. 1993;11(4–5):367–73.
41. Buck MA, Olah TA, Weitzmann CJ, Cooperman BS. Protein estimation by the product of integrated peak area and flow rate. Anal Biochem. 1989;182(2):295–9.
42. Kuipers BJ, Gruppen H. Prediction of molar extinction coefficients of proteins and peptides using UV absorption of the constituent amino acids at 214 nm to enable quantitative reverse phase high-performance liquid chromatography-mass spectrometry analysis. J Agric Food Chem. 2007;55(14):5445–51.
43. Mitchell J, Smith DM, Ashby EC, Bryant WMD. Analytical procedures employing Karl Fischer reagent. IX. Reactions with inorganic oxides and related compounds. Oxidation and reduction reactions. J Am Chem Soc. 1941;63:2927–30.
44. Patel K, Borchardt RT. Chemical pathways of peptide degradation. II. Kinetics of deamidation of an asparaginyl residue in a model hexapeptide. Pharm Res. 1990;7:703–10.
45. Stephenson RC, Clarke S. Succinimide formation from aspartyl and asparaginyl peptides as a model for the spontaneous degradation of proteins. J Biol Chem. 1989;264(11):6164–70.
46. Oliyai C, Patel J, Carr L, Borchardt RT. Solid-state stability of lyophilized formulations of an asparaginyl residue in a model hexapeptide. J Parenteral Sci Technol. 1994;48:67–173.
47. Lai M, Hageman MJ, Schowen RL, Topp EM. Chemical stability of peptides in polymers. 1. Effect of water on peptide deamidation in poly(vinyl alcohol) and poly(vinylpyrrolidone) matrices. J Pharm Sci. 1999;10:1073–80.
48. Song Y, Schowen RL, Borchardt RT, Topp EM. Effect of 'pH' on the rate of asparagine deamidation in polymeric formulations: 'pH'-rate profile. J Pharm Sci. 2001;90:141–56.
49. Capasso S, Balboni G, Di Cerbo P. Effect of lysine residues on the deamidation reaction of asparagine side chains. Biopolymers. 2000;53:213–9.
50. Paranandi MV, Aswad DW. Spontaneous alterations in the covalent structure of synapsin I during *in vitro* aging. Biochem Biophys Res Commun. 1995;212:442–8.
51. Kang HJ, Coulibaly F, Clow F, Proft T, Baker EN. Stabilizing isopeptide bonds revealed in gram-positive bacterial pilus structure. Science. 2007;318:1625–8.
52. Wikoff WR, Liljas L, Duda RL, Tsuruta H, Hendrix RW, Johnson JE. Topologically linked protein rings in the bacteriophage HK97 capsid. Science. 2000;289:2129–33.
53. Dierkes LE, Peebles CL, Firek BA, Hendrix RW, Duda RL. Mutational analysis of a conserved glutamic acid required for self-catalyzed cross-linking of bacteriophage HK97 capsids. J Virol. 2009;83:2088–98.
54. Simons BL, King MC, Cyr T, Hefford MA, Kaplan H. Covalent cross-linking of proteins without chemical reagents. Protein Sci. 2002;11:1558–64.
55. Maroufi B, Ranjbar B, Khajeh K, Naderi-Manesh H, Yaghoubi H. Structural studies of hen egg-white lysozyme dimer: comparison with monomer. Biochim Biophys Acta. 2008;1784:1043–9.
56. Shamblin SL, Hancock BC, Pikal MJ. Coupling between chemical reactivity and structural relaxation in pharmaceutical glasses. Pharm Res. 2006;23:2254–68.
57. Severs JC, Froland WA. Dimerization of a PACAP peptide analogue in DMSO via asparagine and aspartic acid residues. J Pharm Sci. 2008;97:1246–56.